

# NJC

Accepted Manuscript



This is an *Accepted Manuscript*, which has been through the Royal Society of Chemistry peer review process and has been accepted for publication.

*Accepted Manuscripts* are published online shortly after acceptance, before technical editing, formatting and proof reading. Using this free service, authors can make their results available to the community, in citable form, before we publish the edited article. We will replace this *Accepted Manuscript* with the edited and formatted *Advance Article* as soon as it is available.

You can find more information about *Accepted Manuscripts* in the [Information for Authors](#).

Please note that technical editing may introduce minor changes to the text and/or graphics, which may alter content. The journal's standard [Terms & Conditions](#) and the [Ethical guidelines](#) still apply. In no event shall the Royal Society of Chemistry be held responsible for any errors or omissions in this *Accepted Manuscript* or any consequences arising from the use of any information it contains.

## Preparation of disordered carbon from rice husk for lithium-ion batteries

Yi Li<sup>a</sup>, Fengying Wang<sup>a</sup>, Jicai Liang<sup>a</sup>, Xiaoying Hu<sup>b</sup>, and Kaifeng Yu<sup>a\*</sup>Received 00th January 20xx,  
Accepted 00th January 20xx

DOI: 10.1039/x0xx00000x

www.rsc.org/

Rice husk (RH) was employed as the precursor for the preparation of disordered carbon for lithium-ion batteries. Disordered carbon was synthesized by pyrolysis of RH under inert gas atmosphere followed by base treatment to remove the silica fraction. These carbons were characterized through X-ray diffraction (XRD), Brunauer-Emmett-Teller (BET) measurement, Scanning electron microscope (SEM), Raman and Transmission electron microscope (TEM). The effects of reaction temperature with NaOH on the capacity of these carbons were described. These carbons showed a high reversible capacity of 502 mAhg<sup>-1</sup> after 100 cycles at 0.2 C in lithium-ion battery anodes.

Key words: Rice husk; Disordered carbon; Lithium-ion batteries

### 1. Introduction

With the growth of population and economy, energy consumption increases dramatically in the world. So far the world energy sources are mainly dependent on fossil fuels (coal, petroleum, and natural gas). The main issue of using fossil fuels is that they are nonrenewable and produce CO<sub>2</sub> and other greenhouse gases.<sup>1</sup> There is an increasing pressure for almost every manufacturer to go “green” and seek sustainable development, especially for the energy industry that is highly dependent on fossil fuels.<sup>2</sup> Wind and hydropower are renewable sources and friendly to environment, but the facilities for these energy are both high cost. Hence the search for low-cost, clean and renewable energy materials, as well as their related devices, is arousing interest worldwide in recent years.<sup>3,4</sup> Since lithium-ion secondary batteries were commercialized by SONY in 1991, they have become the best portable energy storage devices for the consumer electronics market.<sup>5</sup> The application of lithium batteries is being extended to a variety of consumer and military applications where they are generally considered as one of the most state-of-the-art power devices in conjunction with fuel cells and supercapacitors.<sup>6,7</sup> Due to the low cost, eco-friendliness, high electrical conductivity, good electrocatalytic activity and chemical stability, as well as low electrochemical potential toward lithium intake, carbonaceous materials have been widely studied as anode materials for rechargeable lithium-ion batteries (LIBs).<sup>7</sup>

At present, graphite, a carbonaceous material with the highest degree of graphitization, as a commercial anode material for LIBs possesses the advantages of high coulombic efficiency and good cycle stability.<sup>8,9</sup> However, the low theoretical capacity (372 mAhg<sup>-1</sup>) and poor rate capability of commercialized graphite anode materials cannot meet the ever-increasing energy demands of portable electronics and practical electric vehicles.<sup>10,11</sup> The intense search for alternative anode materials capable of intercalating larger amounts of lithium has led to the synthesis of many unique disordered carbon materials which possess high potential in many applications including adsorption, gas storage, energy storage and conversion.<sup>12</sup> Disordered carbons are widely used as anode materials for

lithium-ion batteries due to stable cycle performance, high specific capacity and negative redox potentials.<sup>13</sup> A variety of carbonaceous materials used as anodes of lithium-ion batteries have been prepared by pyrolysis of biomass precursors such as sugar, cotton fibers, coffee beans, walnuts, rice husk and wood.<sup>5,14</sup> The capacity of such materials is critically dependent on pyrolysis conditions and precursor sources.<sup>15</sup> To lower the cost of raw materials, the selection of precursor has been shifted to natural or agricultural residues in this work.

Recently, as a renewable source, biomasses have attracted much attention for their application in the preparation of disordered carbon. Rice husk (RH) is a kind of agricultural biomass waste in rice-producing countries and has the advantages of being inexpensive and widely available.<sup>16</sup> The annual yield of rice is about 600 million tons in the world, which generates more than 100 million tons of rice husks (RHs).<sup>17,18</sup> RH usually has a light weight, hence, the disposal of RH could be a problem. As a result, a great amount of RHs are burnt through wildfire or post-harvest burning of cultivation fields,<sup>19</sup> which can cause air pollution and resource waste. In some areas, RHs are used for fuel due to their high calorific power. The major components of RH are SiO<sub>2</sub>, cellulose (38%), hemicelluloses (18%), and lignin (22%), which yield carbon when pyrolyzed under inert atmosphere.<sup>17</sup> RHs were the most studied carbon precursors among rice wastes.<sup>19</sup> The processing of preparing disordered carbons from RH involves carbonation, pulverisation, chemical treatment, and activation. Fey's group reported on the use of rice husk as a precursor for the preparation of pyrolytic carbons which used as a negative electrode in Li ion batteries. High insertion capacities of 819 mAh g<sup>-1</sup> was observed for the carbon obtained from rice husk treated with 0.3 M NaOH.<sup>17</sup> In this paper, we report the results of our work on the pyrolytic synthesis of carbons from RH, and their structural and electrochemical characteristics. The RH-derived carbon has advantages like low cost and the raw materials are abundance, and the carbon exhibits stable electrochemical performance. Meanwhile, the process of the preparation of RH-derived carbon in this paper is very simple and low cost.

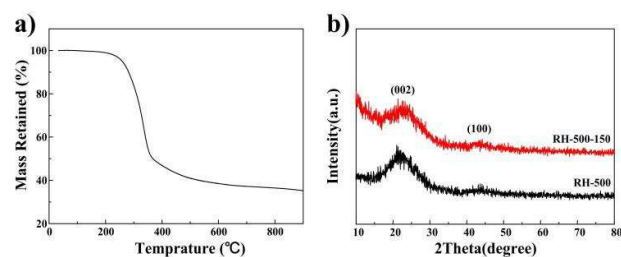


**Figure 1.** a) TG curves of rice husk in nitrogen, b) XRD pattern of RH-500, RH-500-150, respectively.

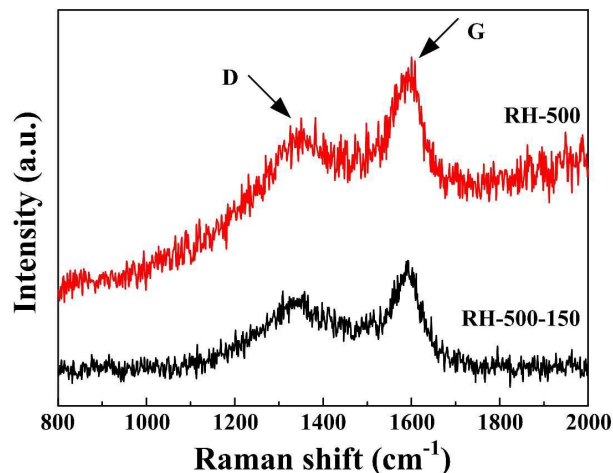


**Figure 2.** Raman spectra of RH-500, RH-500-150, respectively.

## 2. Results and discussion

Fig. 1a displays the TG trace recorded for the RH sample between room temperature and 900 °C at a heating ramp of 5 °C/min in nitrogen. The weight loss observed around 115 °C, which is due to the loss of superficial moisture and other light volatiles from the RHs. The active pyrolysis zone for RHs was between 250 and 380 °C, which is attributed to the evolution of volatiles emanating upon decomposition of primary hemicellulose and cellulose.<sup>14</sup> A third weight loss centered around between about 400 and 500 °C due to the loss of volatile vapors and aromatic condensation processes that are part of the intricate pyrolytic reactions. The decomposition of the precursor is completed around 500 °C and any change that occurs beyond this temperature is attributed to carbon layer organization.<sup>6</sup> The X-ray diffraction patterns of the carbons pyrolyzed at 500 °C are shown in Fig. 1b. The patterns of the two samples show no characteristic peak, indicating that both of the samples exhibit the turbostratic structure of disordered carbon material.<sup>16</sup> The diffraction patterns which give broad peak for the (002) reflection around 22 ° suggest the small domains of coherent and parallel stacking of the graphene sheets. A weak broad peaks corresponding to the (100) reflections can be seen around 44 °, indicating the presence of honeycomb structures formed by sp<sup>2</sup> hybridized carbons.<sup>20</sup> Moreover,

no sharp peaks are observed in the XRD patterns, which indicate their amorphous state.

The Raman spectra of the carbons are shown in Fig. 2. The G-band appearing at 1590 cm<sup>-1</sup> is attributed to the vibration of sp<sup>2</sup>-bonded carbon atoms in a 2D hexagonal lattice, while the peak of the D-band near 1340 cm<sup>-1</sup> is related to edges, other defects, and disordered carbon in the graphitic structure. The I<sub>D</sub>/I<sub>G</sub> intensity ratio of the RH-500-150 is 0.88, which is higher than that of the RH-500 (I<sub>D</sub>/I<sub>G</sub>=0.79). This represents a higher degree of disorder, more edges, and more other defects, which favors an enhanced reversible capacity of the anode.<sup>2,4,5</sup>

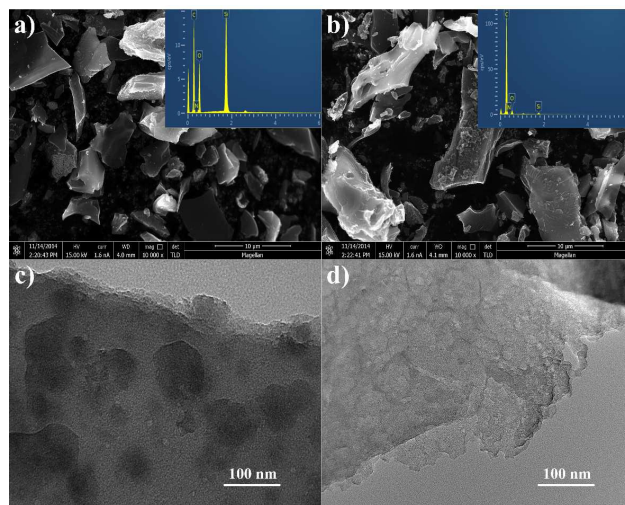


**Figure 3.** (a) and (b) SEM image of RH-500 and RH-500-150, (c) and (d) TEM image of RH-500 and RH-500-150, respectively.

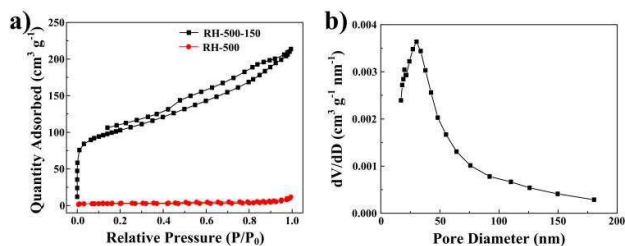


**Figure 4.** (a) Nitrogen adsorption-desorption isotherms of RH-500 and RH-500-150. (b) Pore size distribution of RH-500-150.

The morphology of the samples were characterized by SEM and TEM, the results are shown in Fig. 3. Fig. 3a-b show the SEM and EDS of the samples, it can be seen that there is no obvious evidence of macropore formation. The particles do not have a definite shape for all of the samples. From Fig. 3a, it can be seen that RH-500 sample exhibits a smooth surface, while Fig. 3b shows that the surface of the carbons are relatively rough, mainly due to the surface of the samples are corroded by NaOH solution. From the EDS of the samples, it can be seen that the content of silicon decreased

obviously after base-treatment, which can surmise that the generation of pores due to the removal of  $\text{SiO}_2$ . TEM of RH-500 and RH-500-150 are shown in Fig. 3c-d. From the TEM (Fig. 3c) of RH-500, there is no obvious pore on the surface of RH-500, and the material is composite of flake structure, which form a fraction of macroporous. After treated by NaOH solution, there are large number of mesopores appear on the surface of RH-500-150, and the edge of RH-500-150 is obviously corroded (shown in Fig. 3d). From Fig. 3d, it also can be seen that RH-500-150 is composite of large quantities of flake structure and slit-shaped mesopores due to the removal of  $\text{SiO}_2$ .

Fig. 4a shows the nitrogen adsorption isotherms for RH-500 and RH-500-150. According to the isotherm and the BET surface area value (only  $8.57 \text{ m}^2 \text{ g}^{-1}$ ) of the RH-500 sample, the material consists of non-porous or a fraction of macroporous. After treated by NaOH solution, the RH-500-150 materials exhibit a type-IV isotherm with a type-H4 hysteresis loops and the BET Surface area is increased to  $351.81 \text{ m}^2 \text{ g}^{-1}$ . Type-IV isotherm indicates the existence of mesopores and the type-H4 hysteresis loops suggests the presence of slit-shaped pores and the formation of slits due to the accumulation of flake particles in the materials.<sup>21,22</sup> The pore size distribution of the RH-500-150 is shown in Fig. 4 b, which indicates that the materials are mainly composed of mesopores with a broad pore size distribution in the range of 17-48 nm. Compared to RH-500, RH-500-150 presents higher BET Surface area, which is ascribed to the changes in the pore structure caused by the removal of  $\text{SiO}_2$ . The presence of slit-shaped mesopores in RH-500-150 allows electrolytes for easier and faster penetration, and lithium ions for easier and faster diffusion. The result of nitrogen adsorption-desorption of the carbons is consistent with TEM of the carbons.

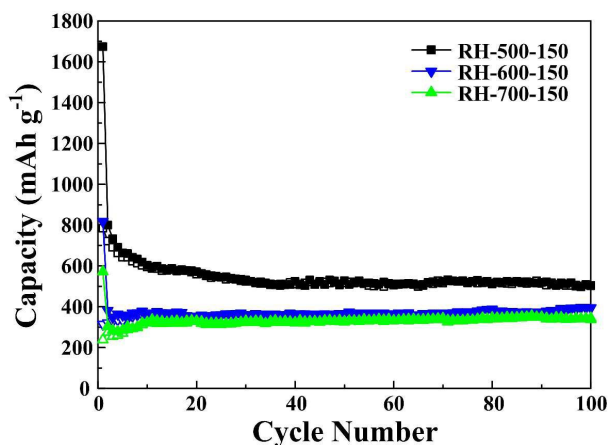


**Figure 5.** Cycling performance profiles of RH-500-150, RH-600-150 and RH-700-150.

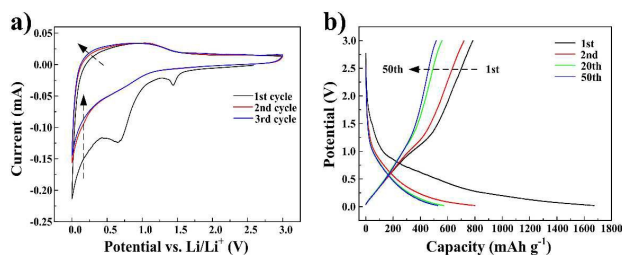


**Figure 6.** (a) Cyclic voltammogram (CV) profiles of RH-500-150, (b) charge-discharge profiles of RH-500-150 respectively.

The electrochemical performances of the carbons as anode materials are investigated. Fig. 5 displays the cycling performance of the RH-derived carbons under different calcination temperature evaluated at a current density of 0.2 C up to 100 cycles. It can be seen that the capacity of the carbons is decreased with the calcination temperature increased, which can be due to the degree of graphitization increased and the collapse of the mesopores under higher calcination temperature. At low temperature ( $500 \text{ }^\circ\text{C}$ ), there is insufficient thermal energy for the graphene sheets to rotate into a parallel alignment, which results in a larger number of non-parallel and unorganized single layers of carbon in the low-temperature carbons. Meanwhile, there are abundant mesopores in the low-temperature carbons. As a result, the sites for lithium insertion are increased. With the temperature increased (increase to  $600$  or  $700 \text{ }^\circ\text{C}$ ), the thermal energies reach values high enough to break the links between adjacent sheets and favor their alignment into parallel orientations, meanwhile the mesopores collapsed and fused into the macropores, which leads to the decrease of the sites for lithium insertion.<sup>5,23</sup>

Fig. 6a shows the cyclic voltammogram (CV) profiles of RH-500-150 electrodes at a scan rate of  $0.1 \text{ mV s}^{-1}$  between 0 and 3.0 V. Two main reduction peaks appear at around 0.65 and 1.45 V during the 1st reduction process for RH-500-150 specimen. The peak at 1.45 V is assigned to the decomposition of the electrolyte and the formation of solid electrolyte interface (SEI) film which caused by the electrolyte decomposition on the active electrode surface.<sup>5,24</sup> The 0.65 V peak is stronger than the one at 1.45 V, which might be due to the reaction of the function groups of the carbon and the lithium ions. No corresponding oxidation peaks are observed in the oxidation segment of the CV profile. Therefore, these two reactions are responsible for the obvious capacity loss in the first cycle.<sup>25</sup> Such peaks disappear after the 1st cycle, and the areas of the cathodic and anodic peaks tend to be the equal to each other, implying the stability of the SEI layer and the structure of the carbon. Fig. 6b shows the discharge/charge profiles of the RH-500-150 at a rate of 0.2 C. The initial discharge capacity of RH-500-150 is  $1647 \text{ mAhg}^{-1}$ , corresponding to Coulombic efficiency of 46.8%. A large irreversible capacity occurs during the 1st cycle for the carbon, which is a phenomenon in carbonaceous electrodes due to the formation of SEI film. In fact, the SEI layer is advantageous, for it prevents the electrolyte from undergoing decomposition on the active electrode.<sup>4</sup> However, the reversible capacity of the carbon becomes stable in the subsequent cycles. According to the SEM,

TEM and BET of RH-500-150 sample, the high first-cycle insertion capacity is likely attributed to the high surface area as well as to the rough surface of the sample and the presence of a large number of slit-shaped mesopores.

Fig.7a displays the cycling performance of the carbons evaluated at a current density of 0.2 C up to 100 cycles. According to the curves, the capacity of RH-500 carbon increases obviously up to 40 cycles, which can be attributed to the activating process of the anodes.<sup>26</sup> It can be due to the SiO<sub>2</sub> in the RH-500 carbon are electrochemically activated during the cycles.<sup>27</sup> Compared with RH-500 anode, the RH-500-150 anode shows excellent cyclability with high capacity. The Coulombic efficiencies were 90% or more and increasing dramatically to 95% after 5 cycles. After 50 cycles, the reversible capacity of the RH-500 anode is maintained at 354 mAh g<sup>-1</sup>, however, the RH-500-150 anode is maintained at 506 mAh g<sup>-1</sup> and the Coulombic efficiency stabilizes at around 99%. After 100 cycles, the reversible capacity of the RH-500-150 anode is 502 mAh g<sup>-1</sup> and the Coulombic efficiency is more than 100%. Furthermore the rate performance of RH-500 and RH-500-150 were investigated at various rates from 0.2 to 10 C (Fig. 7b). At all current rates, RH-500-150 shows a higher capacity than RH-500. At a current rate of 10 C, RH-500-150 electrode shows reversible capacity of 172 mAh g<sup>-1</sup>, whereas the capacity of RH-500 is as low as 21 mAh g<sup>-1</sup>. The reversible capacity of 657 mAh g<sup>-1</sup> is restored when the current density is reversed to 0.2 C, demonstrating the excellent rate performance of RH-500-150. The reversible capacity of RH-500-150 is increased dramatically when the current density is reversed to 0.2 C due to the the activating process of the anodes. The high initial reversible and irreversible capacities of the RH-derived carbons are attributed to the high H/C ratios (Table 1) since Li atoms can bind in the vicinity of the H atoms in the

hydrogen-containing carbons.<sup>4,6</sup> The presence of a large number of nanopores and high surface areas with reactive functional groups that provide ample sites for passivation also play an important role in the high reversible capacities.<sup>6</sup>

Although the RH-derived carbon exhibits high irreversible capacity, the carbon has advantages like low cost and the raw materials are abundance, and the carbon possesses stable electrochemical performance.

### 3. Conclusions

In summary, disordered pyrolytic carbons derived from RH have been shown to possess high capacities for lithium intake. The treatment of the carbon with 2 mol L<sup>-1</sup> NaOH solution at 150 °C for 3 h results in carbon materials with a 33-fold increase in surface area, and the initial discharge capacity of 1647 mAh g<sup>-1</sup> at 0.2C in lithium-ion battery anodes. These carbons showed a high reversible capacity of 502 mAh g<sup>-1</sup> after 100 cycles at a current density of 0.2 C. The high capacities in these disordered carbons are believed to the binding of lithium on extra surfaces of the single layers of carbon and in the nanocavities. Despite these carbons exhibit high capacities, their high irreversible capacities and continued loss in capacity with cycling is a major concern for the applications in lithium-ion batteries. The preparation process of the disordered carbon still need to be further refined to lower the irreversibility capacity loss and to increase cycle life. The simple and low-cost synthesis procedure described here will open new avenues for the preparation of carbon electrode materials.

### 4. Experimental section

#### 4.1 Preparation of disordered carbon

Carbon samples for this work were synthesized as described below. The raw material was obtained from a local rice mill and thoroughly washed with deionized water to remove adhering soil and clay, then dried in an oven over night. About 7 grams of the dried husk was transferred into a horizontal tube furnace, which was then purged with nitrogen for 30 min. The tube was heated at a heating ramp of 5 °C /min in a nitrogen atmosphere and was held at 500 °C for 3 h. After natural cooling to room temperature, the black residues (about 2.5 g) were ground into a fine powders and then refluxed with 2 mol L<sup>-1</sup> HCl solution at 80 °C in a water bath for an hour. After leaching, the specimens were thoroughly washed with deionized water until the filtrate was free from acid, the water in the sample was allowed to evaporate in an oven over night. The dried samples denoted as RH-500 were treated with 2 mol L<sup>-1</sup> NaOH solution through a hydrothermal method to remove silica from RH in a reactor at 150 °C for 3 h. After leaching, the samples were thoroughly washed with deionized water to remove the activating agent until pH 7, and were dried in an oven. The final products were denoted as RH-500-150. In order to have a better understanding of the electrochemical performance of RHs, the RHs were treated under different calcination temperature (600 °C and 700 °C ). The following processes are the same as

**Table 1.** Elemental analysis and contents of RH-500 and RH-500-150.

Sample	Percentage composition			
	C%	H%	N%	H/C
RH-500	52.29	1.577	0.50	0.362
RH-500-150	84.66	2.077	0.96	0.294

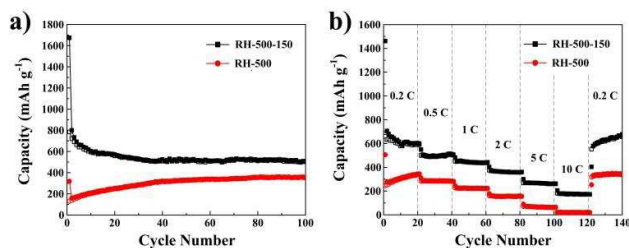


**Figure 7.** (a) Cycling performance profiles of RH-500 and RH-500-150, (b) rate performance of RH-500 and RH-500-150.

described above. The final products were denoted as RH-600-150 and RH-700-150, respectively.

#### 4.2 General Characterization

Powder X-ray diffractometry was performed (Siemens D 5000 X-ray diffractometer) with nickel-filtered Cu K $\alpha$  radiation. The data were collected between scattering angles ( $2\theta$ ) of 10 ° and 80 ° ( $2\theta$ ) in steps of 0.05 °. Raman spectra were recorded on Renishaw inVia. Morphology of the disordered carbons was observed by scanning electron microscopy (SEM) and energy dispersive spectrometer (EDS) with a field-emission-scanning electron microscope (JEOL JSM-6700F). The specific surface area and pore size distribution of the carbons were measured by nitrogen adsorption-desorption measurement (Micromeritics, ASAP 2420). The microstructures of the carbons were examined by transmission electron microscope (JEM-2100F). The samples for TEM studies were prepared by dispersing powders of the products in ethanol, placing a drop of the clear solution on a carbon coated copper grid and subsequent drying. Element analyses were performed on a FlashEA1112 spectrometer.

#### 4.3 Electrochemical measurements

The carbon electrodes for the cells were fabricated on a weight basis of 85 wt.% of the RH-derived carbon, 5 wt.% of carbon black and 10 wt.% PVDF. Excess N-methyl-2-pyrrolidone (NMP) was used and the mixture was stirred at least 5 h until the paste achieved a smooth syrupy viscosity, coating copper foil with the mixed slurry. After dried at 120 °C in a vacuum oven for 12 h, punching out circular discs, the diameter of the circular discs was 10 mm. The carbon electrodes were coupled with lithium metal in the coin cell, with a 1 mol L<sup>-1</sup> solution of LiPF<sub>6</sub> in a 1:1 (v/v) mixture of EC-DEC. All cells were assembled into 2025 button cells in an argon-filled glovebox with moisture and oxygen levels of less than 1 ppm. Galvanostatic charge-discharge profiles were recorded between 0.02 and 3.0 V at a 0.2 C (1 C = 372 mAhg<sup>-1</sup>) rate on a LAND (CT2001A) multi-channel battery tester. The cyclic voltammetry test was performed on an electrochemical workstation (CHI660C) within a voltage window of 0-3.0 V and at a scan rate of 0.1 mVs<sup>-1</sup>.

#### Acknowledgements

The work is supported by the Key Scientific and Technological Project of Jilin Province, Project Grant No. 20140204052GX; Open Project of the State Key Laboratory of Inorganic Synthesis and Preparative Chemistry, College of Chemistry, Jilin University (No. 201505).

#### Notes and references

<sup>a</sup>Key Laboratory of automobile Materials, Ministry of Education, and College of Materials Science and Engineering, Jilin University, Changchun 130025 [yukf@jlu.edu.cn](mailto:yukf@jlu.edu.cn)

<sup>b</sup>College of Scienc, Changchun University, Changchun

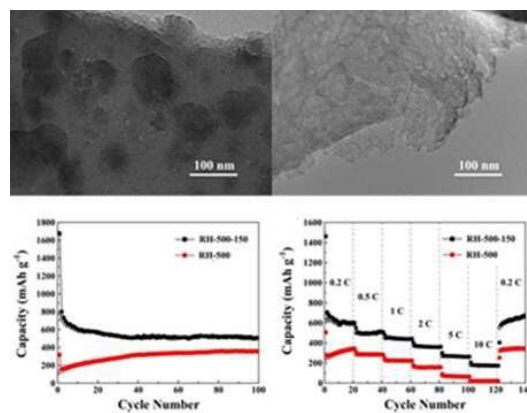
‡ Footnotes relating to the main text should appear here. These might include comments relevant to but not central to the matter

under discussion, limited experimental and spectral data, and crystallographic data.

§

§§

- P. Poudel, Q. Qiao, *NANO ENERGY*, 2014, **4**, 157-175.
- S. X. Wang, L. P. Yang, *ACS Applied Materials & Interfaces*, 2013, **5**, 12275-12282.
- Y. Q. Sun, Q. Wu, G. Q. Shi, *Energy Environ. Sci.*, 2011, **4**, 1113-1132.
- L. Chen, Y. Zhang, C. Lin, *Journal of Materials Chemistry A*, 2014, **25**, 9684-9690.
- S. Han, D. Jung, J. Jeong, *Chemical Engineering Journal*, 2014, **254**, 597-604.
- Yun Ju Hwang, S.K. Jeong, J.S. Shin, K. S. Nahm, *Journal of Alloys and Compounds*, 2008, **448**, 141-147.
- X. L. Wu, L. L. Chen, S. Xin, *ChemSusChem*, 2010, **3**, 703-707.
- R. C. Lee, Y. P. Lin, Y. T. Weng, *Journal of Power Sources*, 2014, **253**, 373-380.
- P. Adelhelm, Y. S. Hu, B. M. Smarsly, *Advanced Materials*, 2007, **19**, 4012-4017.
- F. Han, W. C. Li, D. Li, *Journal of Energy Chemistry*, 2013, **22**, 329-335.
- H. L. Lv, S. Qiu, G. X. Lu, *Electrochimica Acta*, 2015, **151**, 214-221.
- Z. X. Wu, D. Y. Zhao, *Chemical Communications*, 2011, **47**, 3332-3338.
- Z. X. Wu, W. Li, Y. Y. Xia, P. Webley, *Journal of Materials Chemistry*, 2012, **22**, 8835-8845.
- G. T. Fey, Y. Cho, C. Chen, T. P. Kumar, *Pure & Applied Chemistry*, 2010, **82**, 2157-2165.
- G. T. Fey, C. Chen, *Journal of Power Sources*, 2001, **97-98**, 47-51.
- G. Q. Wang, D. L. Wang, S. Kuang, *Renewable Energy*, 2014, **63**, 708-714.
- L. P. Wang, Z. Schnepf, M. M. Titirici, *Journal of Materials Chemistry A*, 2013, **17**, 5269-5273.
- N. Liu, K. F. Huo, M. T. McDowell, *Scientific Reports*, 2013, **3**, 24-29.
- A. H. Basta, V. Fierro, H. El-Saied, *Bioresource technology*, 2009, **100**, 3941-3947.
- A. M. Stephan, T. P. Kumar, R. Ramesh, *Materials Science and Engineering: A*, 2006, **430**, 132-137.
- K. T. Lee, J. C. Lytle, N. S. Ergang, *Advanced Functional Materials*, 2005, **15**, 547-556.
- J. Liu, Y. Wen, Y. Wang, P. A. Aken, *Advanced Materials*, 2014, **26**, 6025-6030.
- G. T. K. Fey, D. C. Lee, Y. Y. Lin, *Synthetic metals*, 2003, **139**, 71-80.
- B. Xu, L. Shi, X. Guo, *Electrochimica Acta*, 2011, **56**, 6464-6468.
- F. D. Han, Y. J. Bai, R. Liu, *Advanced Energy Materials*, 2011, **1**, 798-801.
- L. Qie, W. M. Chen, Z. H. Wang, *Advanced Materials*, 2012, **24**, 2047-2050.
- L. Wang, J. Xue, B. Gao, *RSC Advances*, 2014, **4**, 64744-64746.



The RH-derived carbon exhibits stable electrochemical performance. Meanwhile, the process of the preparation is very simple and low cost.